ARTICLES

Efficiency of Charge Transport in a Polypeptide Chain: The Hydrated System†

Sheh-Yi Sheu,*,‡ Dah-Yen Yang,*,§ H. L. Selzle,|| and E. W. Schlag*,||

Department of Life Science, National Yang-Ming University, Taipei 112, Taiwan, Institute of Atomic and Molecular Science, Academia Sinica, Taipei 106, Taiwan, and Institut fuer Physikalische und Theoretische Chemie, TU-Muenchen, 85747 Garching, Lichtenbergstrasse 4, Germany

Received: March 25, 2002; In Final Form: July 9, 2002

In our previous work we have introduced a bifunctional model to predict the otherwise surprising charge migration in peptides and their chemical reactivity. Such transfer of charge and distal reactivity is often found to occur a long distance from the original site of excitation and is typical in biological signal transduction. This model introduced the subject of reactivity at a distance, in contrast to classical local reaction theories. Our model was initiated by our experimental observation of extremely efficient charge transport in peptides over substantial distances, subject to certain energetic rules, but now survives the introduction of the aqueous medium. The question we wish to study in this paper is the effect of a water environment on such an isolated system. Experimentally it is known that this effect is enormous, in that the charge in the water environment decays over a characteristic distance of only some 1 Å, whereas in our isolated peptide system there is very little attenuation observed. We here do extensive molecular dynamics calculations in the presence of 611 water molecules and demonstrate that our original mechanism survives entering the liquid phase but that the effect of the water is to create a hydrophobic jacket around the peptide that seriously constrains the motion of the peptide. Such motion in the peptide is an essential element in our bifunctional model. In fact when we now calculate the efficiencies in water, we obtain a value near 2.4%, which translates into an exponential β factor of 1 $Å^{-1}$, which agrees with the value experimentally observed for charge transport of β-sheet protein charges in water. Hence, even though the experimental results in the gas phase and in water differ by some orders of magnitude, our bifunctional model is able to encompass both extreme situations, the isolated system and the peptide in the water environment. In both cases the calculations agree with the experimental results.

Introduction

Chemical reactivity at a distance is a common but incompletely understood process in biological processes. In such processes the site of energy deposition and the site of chemical reaction are far removed from each other; such systems are typical for signal transport in biological systems. Such a notion of reactivity differs from the more classical reaction rate theories in which energy deposition, after some rearrangement, leads to reaction at a site perhaps only a few bonds away from the site of excitation.[1]

In previous work we showed that a typical form of long-range transport of such energy can be via a charge traveling down the peptide chain. Such a charge transport through polypeptide chains is not a self-evident process. Peptides have properties, however, which make them almost uniquely able for such a long-range transport. We investigated this process originally for isolated peptides in the gas phase where we were interested in exploring the purely molecular properties of this process and found charge transport to be extremely efficient. We developed a model to explain this very facile charge transport and found that this model also conformed with recent experiments on the proteomics of large systems studied with mass spectrometry.[2−6] The distal transport of charge is of broad consequence in biological systems—"the flow of electrons in oxidation−reduction reactions is responsible directly or indirectly for all of the work done by living organisms".[7] Though charge transport in a protein polypeptide chain has been extensively studied, its detailed mechanism remains a central question.

With a simple model including the detailed protein structure and the dynamic driving force, in our previous work,[8−10] we have demonstrated that not only charge but also chemical reaction can occur at a considerable distance away from where the system is initially excited. Some proteins facilitate the charge transport process, and others do not. More to the point some modifications in the protein chain interrupt the process as in a switch. We have developed some rules for this previously. As a result, proteins can act as molecular wires and even be logic gates triggered by the charge transport process and triggered with very small energy such as found in a redox process. The previous charge transport mechanism is based upon the nonadiabatic ET rate[11,12] between segments, traveling along the

* Corresponding authors. E-mail: S.-Y.S., sysheu@ym.edu.tw; E.W.S., schlag@ch.tum.de. E-mail: D.-Y.Y., dyyang@po.iams.sinica.edu.tw.

† Dedicated to Prof. Friedrich Doerr on the occasion of his 80th birthday.

‡ National Yang-Ming University.

§ Academia Sinica.

|| TU-Muenchen.

10.1021/jp020799w CCC: $22.00
Published on Web 09/13/2002

protein backbone. Instead we proposed a bifunctional model which includes two states, a "rest" and "fire" mechanism for this protein charge transport and reactivity. Our model includes essential protein dynamic effects in addition to electronic effects to facilitate charge transfer in proteins. Hence, the basic concept relies on the fundamental structure and dynamic information which is stored in the Ramachandran plot.[13] Motion of the rotors around a C_α-hinge is taken as a virtual ballistic particle moving inside a subregion called the Baranov−Schlag (BS) box[9] similar to the Ramachandran plot. Escaping from this BS box with a gate on its perimeter is dominated by an entropy barrier. Therefore, the entire charge-transfer process is entropy driven.

In a gas phase system, a molecular dynamics (MD) simulation result shows that using our bifunctional model the charge migrates along the polypeptide chain very efficiently as also observed in mass spectroscopy.[2−6] The flow of charge in isolated peptides is observed to be an extremely efficient transport mechanism, nearly 100% proceeding to the final site, starting from the C-terminus. We now want to test this detailed mechanism in the more typical aqueous environment where the efficiency is experimentally found to be extremely small, in that the charge decays to 1/e in as little as 1 Å. Hence we have 2 orders of magnitude in range of transport to be accounted for as a result of the change of medium. In this paper, we apply our bifunctional model to charge transport in a solvated polypeptide system. The basic idea of the charge transport process is that the charge is initially located at the C-side of the C_α-hinge. This can be pictured as a virtual Brownian particle moving around the BS box inside the Ramachandran plot until it reaches the exit gate. The successful escape should be counted before vibrational modes and solvent modes set in. In other words, we only consider the O−O atoms collision within the energy dissipation time. This we published previously as an analytic theory as well as extensive MD calculations presented as a mean first passage time between residues of some 160−180 fs.[8−10]

The interesting new sidelight on these MD calculations is that we find that not all initial starting configurations of the calculation lead to a firing state, but in fact a fraction of initial states are dissipated, leading to an efficiency in the process of less than unity. Such an inefficiency in charge transport is experimentally well-known[14−23] and leads to β values in the efficiency Y of charge transfer with distance

$$Y = Ae^{-\beta R} \tag{1}$$

with typical values in condensed media of β near 1.0 Å^{-1}. Here A is the prefactor.

In a superexchange model,[24] the electron-transfer rate is proportional to a distance-dependent exponential form $Ae^{-\beta R}$, where the β-value is the distance decay factor and R is the charge transport distance between redox active sites. Similarly such a distance dependence is observed for charge transport in DNA and is between 0.1 and 1.40 Å^{-1}. For the α-helix such as myoglobin in water, the β-value is 1.3 Å^{-1}. Azurin as a β-sheet shows a β-value of 1.0 Å^{-1}. Often eq 1 is considered to be directly connected only with the superexchange model. This is an overstringent view. We show here that our special hopping model also is of this form.

Theoretical prediction of the β-value in the aqueous medium has been investigated by Beratan and Onuchic et al.[22,23] They used Marcus rate theory and combined it with a tunneling pathway model in protein to obtain the β-value.

We suggest a unified model which includes the near 100% efficiency observed by us in the isolated molecule and also explain the β-values generally observed in water of near unity. Such a β-value near unity translates in our model to a single hopping efficiency of only some 3%.

In this paper, we extend our bifunctional model to include efficiencies which we obtain also from MD calculations and thus compute the theoretically predicted β-value which we then compare to experimental data. As an important first step we have to depart from the global motions and use a program which includes the energy with well-defined parameters locally in the chain. (This was achieved by modifications in the CHARMM program.[25]) We term this a single-site MD calculation. This is highly desirable to avoid interference from other energy sources in the global model. We introduce this new MD method of single-site heating which makes the study of these new effects possible and which is close to the physical model we wish to study. The final result confirms our bifunctional model and dynamics contribution to protein charge transport in the gas phase and extends these to include the low efficiency observed in water. These efficiencies from this new model thus encompass both limits, gas phase and water.

Bifunctional Model: Local Heating, Energy Dissipation Time. and Efficiency

In this section, we shall describe the connection between our bifunctional model and β-value. A general procedure is described in the following:

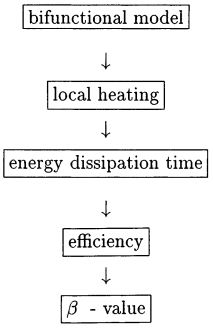

Let us consider a charge transport along a polypeptide chain. At each C_α atom, the torsional angles ψ and ϕ are constrained in the Ramachandran plot (see Figure 1a). Two of the vectors such as $\overrightarrow{C_\alpha N}$ and $\overrightarrow{C_\alpha C}$ of the C_α atom form a hinge. The charge is transported from the C-side of the polypeptide chain to the N-side. Before the charge is transported, it waits in the C-side of the C_α atom until the O−O atoms between two connected amino acids collide, i.e., close to some certain distance in our case. This kind of rotational motion of ψ and ϕ angles is similar to a Brownian particle moving inside a 2D box with a static gate where the O−O atoms collide with each other and charge starts to transfer. It is clear that our bifunctional model exhibits an entropy-driven charge transport process.

In the local heating method described here, the charge transport process is considered to involve a rotational mode which has been turned on before the vibrational mode sets in. In other words, the rotational energy does not dissipate into the heat bath. The chain ionization potential (IP) descending along the polypeptide chain prevents the charge from back-flowing. We hence heat up the rotational mode of the ϕ-angle on the C-side of the C_α- hinge. It is useful to define the $\overrightarrow{C_\alpha N}$ and $\overrightarrow{NX}$ vectors from the C_α atom to the N atom and from the N atom to the X atom, respectively. Note that the X atom can be any atom bound to the N atom (see Figure 1a). We may define the vector orthogonal to the $\overrightarrow{C_\alpha N}$ axis by $\overrightarrow{NX}_\perp = \overrightarrow{NX} \sin\theta$, where

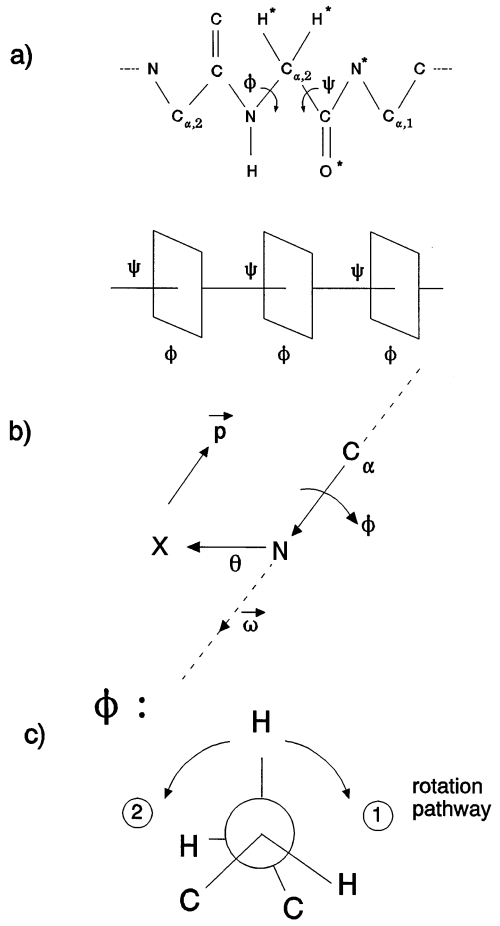

Figure 1. Scheme for bifunctional model. (a) Sequential hopping between residues. At each C_α atom, there are a pair of torsional angles ψ and ϕ. These perform the so-called C_α-hinge. Below the polypeptide chain, we show the corresponding BS box with a gate. (c) Rotation pathway. Before the charge is transported, it waits in the N-side of the C_α-hinge. Our local heating procedure enhances the rotation frequency in any of the rotation pathways. (b) Local heating procedure. Here we define the vectors $\vec{\omega}$ and $\vec{p}$.

$\cos\theta = (\overrightarrow{C_\alpha N}\cdot\overrightarrow{NX})/(|\overrightarrow{C_\alpha N}||\overrightarrow{NX}|)$. Therefore there remain two unknown vectors which need to be solved (see Figure 1b). The first one is the torsional angular momentum. It is useful to set its rotation axis along the $\overrightarrow{C_\alpha N}$ vector by $\omega = [(\overrightarrow{C_\alpha N})/(|\overrightarrow{C_\alpha N}|)]\omega$, where we provide a rotation energy $(1/2)I\omega^2$ (in units of thermal energy) to the X atom and I is the inertial moment. Hence, we obtain the relationship of $\overrightarrow{NX}_\perp \times \vec{p} = \vec{\omega}$. The other one is the excited angular velocity of the X atom $\vec{p}$ which should be tangential. According to the vector relationship $\vec{p}/|\vec{p}| = (\overrightarrow{NX}_\perp \times \overrightarrow{C_\alpha N})/(|\overrightarrow{NX}_\perp||\overrightarrow{C_\alpha N}|)$, we find that the magnitude of $\vec{p}$ is equal to $\overrightarrow{NX}_\perp \times \vec{\omega}\cdot|(\overrightarrow{NX}_\perp\cdot\overrightarrow{C_\alpha N})/(|\overrightarrow{NX}_\perp||\overrightarrow{C_\alpha N}|)|^{-1}$. Note that the unit of unit of ω has to be changed into MD velocity. In our MD simulation, we provide a charge energy ($E = (1/2)I\omega^2$), which is ca. E_{2000K} to the atoms attached to the ϕ axis, i.e., C, O, and three H atoms. Here the charge energy or excitation energy E is in unit of thermal energy. The remaining atoms in the polypeptide chain are still kept at 300 K as background temperature. Typically, in each simulation, 3000 configurations have been chosen. Only part of the configurations have a successful O−O collision, i.e., O and O atoms come close to a certain distance, say 2.8 Å. Hence we define the efficiency as

$$\text{efficiency} = \text{successful configurations within energy dissipation time scale/total configurations} \quad (2)$$

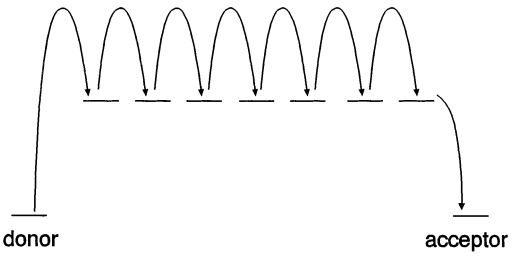

Figure 2. Superexchange model. The charge is conducted from acceptor to donor through the bridge.

With the preceding local heating method, we first determine the first passage time distribution (FPTD) of O−O atoms collision. On the basis of this FPTD, we can read the energy dissipation time, i.e., τ_{diss}. Then, we count the successful O−O contact within the time scale τ_{diss} to obtain the efficiency. The connection between efficiency and the β-value will be presented in the next section.

According to the single-site heating procedure, the charge energy may propagate along the polypeptide chain until its energy is dissipated into the heat bath. In the gas phase, the rotational energy dissipates into the polyatomic vibration mode with a time scale $\tau_{diss} \approx 1$ ps. In the solvated phase, there exists a solvent shell surrounding the polypeptide chain which generates a barrel and prevents the O−O atoms from colliding. This means that the collision between the carbonyl group of both sides of C_α -hinge and solvent molecules provides another channel for energy dissipation. There one may have at least two dissipation time scales while the solvent dissipation time scale is shorter than vibrational dissipation time scale.

Efficiency and β-Value

In this section, we study the charge transport efficiency in our bifunctional model. The typical picture for charge transfer is that the rate or efficiency goes as $Ae^{-\beta R}$. This is naturally justified for a superexchange[24,26] or tunneling mechanism in which the level structure is shown in Figure 2, where the system has tunneled through a barrier with thickness R.

Alternatively consider the peptide as a system of links or pearls (individual amino acids) on a string in which at the juncture we induce transfer to the next link or lose energy to the phonons. The distance between the pearls, for a typical peptide like angiotensin, is some 3.7 ± 0.1 Å.

This coupling could be a conical intersection involving 2−3 vibrations. At this point we may have some loss to the phonon bath due to the involvement of these 2−3 vibrations. Hence, at the link juncture we postulate a rate constant for charge transfer k_t and a rate constant for loss to the bath k_b. The fraction that continues as charge is thus $k_t/(k_t + k_b)$ after n links in the peptide; the fraction of charge that survives is

$$\left|\frac{k_t}{k_t + k_b}\right|^n \quad (3)$$

We can also state the survival more typically as $e^{-\beta n}$, where β is typically 0.8−1.4 Å^{-1}. A very efficient transfer is in DNA[20−23] where $\beta = 0.2$ Å^{-1}. This $e^{-\beta n}$ means that we have e^{-1} for 5 Å^{-1} whereas for the typical $\beta = 1.0$ Å^{-1} we have e^{-1} already for 1 Å; i.e., the former case has better transfer. The typical interlink distance in angiotensin is 3.7 ± 0.1 Å/unit. The total length of the chain is

$$R = 3.7n \quad (4)$$

or $e^{-\beta R} = e^{-3.7\beta n}$. Since $a^n = e^{n \ln a}$, where $a = k_t/(k_t + k_b) =$ efficiency in eq 2, thus eq 3 becomes $e^{n \ln a}$, where by comparison with eq 4

$$\beta = -\frac{\ln a}{3.7} \tag{5}$$

For $\beta = 1.4$ Å^{-1} one gets $\ln(1 + (k_b/k_t)) = 5.18$ or $k_b/k_t = 177$. This means less than 1% charge transfer at each step. The rest is lost to the phonon or heat bath. Similarly for $\beta = 0.2$ Å^{-1},[27-30] the ratio of k_b/k_t is 1.1. Now both processes are equally fast. Note that over the small range of β from 0.2 to 1.4 Å^{-1} the ratio of rates goes from 50:50 to a transfer rate of only 0.6% of the total.

Molecular Dynamics Simulation Results

In our previous work, we found that the FPTD of $(Gly)_3$ is similar to $(Phe)_3$. Therefore, the size of side chain attached to the polypeptide backbone does not substantially influence the FPTD. Hence, in this work, we simulate a polypeptide chain with 20 residues cut from myoglobin native structure, i.e., $(Mb)_{20}$.

First, we show the equivalence of efficiency between single-site local heating and global heating procedures. Of course, the advantage of the local heating method is that, for a long polypeptide chain, real protein and solvated system, there is no strong disturbance of the environmental system. In general, we find, in a vacuum, local heating and global heating methods provide the same efficiency below 1 ps. In the global heating method in ref 8, we heat up all of the atoms in the polypeptide chain to 2000 K, though there are large scale fluctuations of the polypeptide chain. Most of the fluctuation modes are just phonon modes. We fit the stochastic motion of ψ and ϕ angles by using a Gaussian distribution function and the phonon modes by a sigmoid curve. The efficiency of the successful O−O collision, i.e., area below the Gaussian distribution curve, is ca. 0.84. However, the efficiency in global heating at 2000 K is ca. 0.26. Hence, the real efficiency of global heating is equal to $0.26 \times 0.84 = 0.22$. Now let us turn to examine the local heating of $(Gly)_3$ in a vacuum. Recall that the background temperature of the polypeptide chain is 300 K. The MD simulation of the local heating with an excitation energy E_{2000K} has the efficiency equal to 0.19. So the local heating energy of the ϕ angle (or $\overrightarrow{CN}$ axis) is E_{2300K}. The ratio of the excitation energy is 0.87 (=2000/2300). We should reduce the total efficiency by a temperature factor for the global heating with $0.22 \times 0.87 = 0.19$. This is almost exactly the same efficiency as the local heating result. Note that in the global heating procedure both of the ψ and ϕ angles are heated. However, in the local heating procedure, we only allow the ϕ angle to be excited. Therefore, we find that the efficiency of local heating of $(Gly)_3$ in a vacuum is the same as the efficiency of global heating. In other words, the sigmoid part in Figure 2 of ref 8 actually reflects the correct FPTDs. In our local heating MD simulation result (see Figure 3), on the contrary the long time tail is almost totally absent. Hence, we find that the extra high-temperature phonon modes or large scale fluctuations do not influence the stochastic motion inside the BS box. This confirms the similarity of the two methods at early times, as one might expect.

Solvent Dissipation Time. In our previous paper, we locally heat up the ψ angle of the medial Gly of $(Gly)_3$ dissolved in water with an excitation energy E_{1667K} which is ca. 150 meV. This corresponds to a charge transport direction from the C-side to the N-side. During the MD simulation, the first collision between O−O atoms within 2.8 Å is counted as a successful run. The molecular structure calculation is carried out in the presence of 611 water molecules. After some picoseconds the equilibrium structure shown in Figure 4 is generated. From this it is seen that water makes a hydrophobic jacket around the peptide with a barrel shape of some 6 Å diameter. This water barrel is expected to seriously impede the O−O collisions required for charge transport. The MD calculations confirm this and reflect a very low efficiency as a result of the water barrel. Hence we have the interesting if not at first surprising result that water, far from assisting charge transport here, seriously impedes the charge transport process in this model. It is of interest that this strong impediment to charge transfer caused by the water barrel reduces the efficiency in the MD calculation to below 1% at each site. This generates a β-value according to eq 5 of 1.3 Å^{-1}, a value in astonishing agreement with experiment. This appears to point to a water barrel effect on charge transport in proteins. The inner diameter of the water barrel is ca. 6.0 Å. Within such a short distance between the O atom and the water molecule, in Figure 5, a first passage time distribution curve shows a quick energy dissipation process within 500 fs. The thermal fluctuation and protein−solvent collision produce the noise part and will not be counted as efficiency. We estimate the successful run with efficiency equal to 0.008, i.e., the β-value = 1.3 Å^{-1}. We fit our β-value by labeling the local efficiency with p_y^x, where x is the local heating site and y is the residue site. Since our local heating direction is, for example, from the C-side of the C_α-hinge toward the N-side of the polypeptide chain, we take the geometric mean

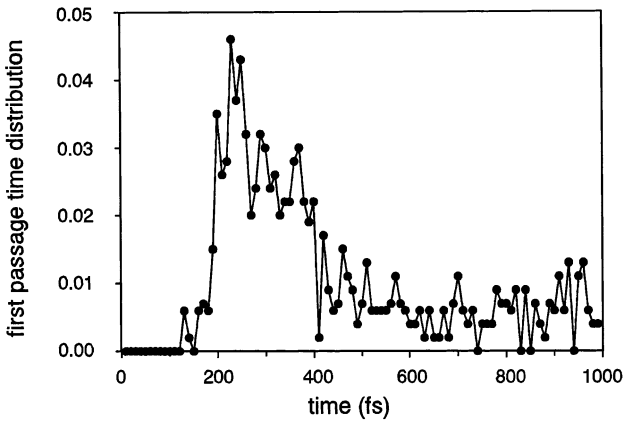

Figure 3. First passage time distribution for polypeptide chain $(Gly)_3$. We locally excite the atoms attached to the ψ-angle of the $C_{\alpha,2}$-hinge of $(Gly)_3$ in a vacuum. In this simulation, we choose 3000 configurations. The thermal nose part is depressed.

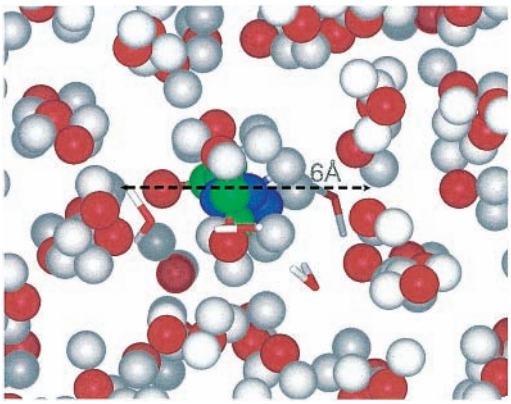

Figure 4. $(Gly)_3$ in a water cavity. The distance between O atom and a water molecule is ca. 6.0 Å.

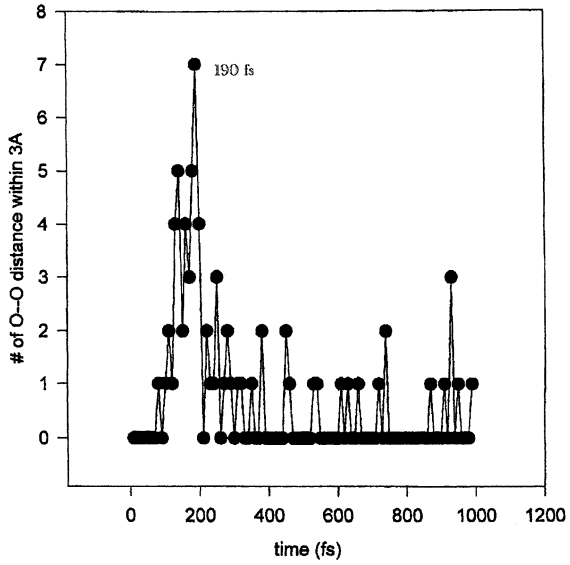

Figure 5. First passage time distribution vs time. A short $(Gly)_3$ polypeptide chain is dissolved in the water system. In this FPTD curve its probability increases after 500 fs; i.e., energy starts to dissipate.

TABLE 1: Efficiency of MB_{20}[a] in the Water System[b] (Local Heating Site 10)[a]

residue no.	efficiency	residue no.	efficiency
1	0.018	11	0.24
2	0.041	12	0.15
3	0.087	13	0.11
4	0.16	14	0.064
5	0.11	15	0.08
6	0.18	16	0.098
7	0.020	17	0.046
8	0.035	18	0.196
9	0.29	19	0.20
10	0.014		

[a] Polypeptide sequence: $Glu_1-Asp_2-Leu_3-Lys_4-Lys_5-Hsd_6-Gly_7-Val_8-Thr_9-Val_{10}-Leu_{11}-Thr_{12}-Ala_{13}-Leu_{14}-Gly_{15}-Ala_{16}-Ile_{17}-Leu_{18}-Lys_{19}-Lys_{20}$. [b] In this simulation there are 611 H_2O's.

TABLE 2: Efficiency of MB_{20} in the Water System (Local Heating Site 8)[a]

residue no.	efficiency	residue no.	efficiency
1	0.042	11	0.14
2	0.042	12	0.023
3	0.025	13	0.040
4	0.127	14	0.062
5	0.079	15	0.087
6	0.21	16	0.042
7	0.25	17	0.11
8	0.44	18	0.13
9	0.066	19	0.15
10	0.091		

[a] Here the simulation condition is the same as in Table 1. Only the local heating site is now at residue Val_8.

such as $p_{10}{}^{10}p_9{}^{10} \times \ldots \times p_1{}^{10} = A \exp(-\beta \times 3.7 \times 10) = 5.78 \times 10^{-13}$ in Table 1. On the other hand, we also have the geometric mean for the case with local heating site 8, i.e., $p_8{}^8p_7{}^8 \times \ldots \times p_1{}^8 = A \exp(-\beta \times 3.7 \times 8) = 1.022 \times 10^{-8}$ in Table 2. The ratio for these two different local heating site situations gives a β-value equal to 1.32 $Å^{-1}$. The other extreme case, gas phase, in ref 10, shows a β-value equal to 1.158 $Å^{-1}$ by using the same geometric mean method here.

Polarization interactions with water have not been considered here, and these could further modify the above efficiencies.[31,32]

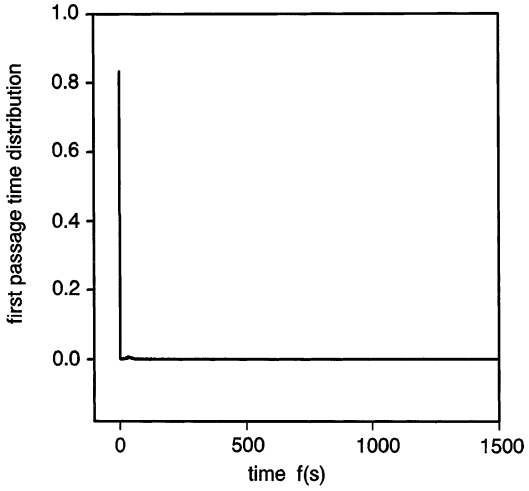

Figure 6. First passage time distribution vs time. The FPTD curve of residue 83 in azurin shows a sharp peak. This FPTD curve is counted for O−O distance larger than 4.0 Å. The β-structure in azurin is quite rigid.

Secondary Structures

We have shown above that the MFPTs and efficiencies/site appear to be robust even when the residues are changed and the length of the chain is changed. It even works for 20 residue portions taken from a natural protein, myoglobin. The next question one might ask is if these results are also the same for different secondary structures. Would we expect the same result for β-sheets and α-helices?

In this section we show that these secondary structures now have important additional effects on our transport model. In particular we will see that again the mean first passage time is robust, as it must be if we want to maintain this high speed, which we think is essential for this model to avoid dissipation. Interestingly though the efficiencies are different for the native α-helix as compared to the β-sheet. The proximity of the groups in the α-helix are very close to the "firing" position; hence, only very small motions are needed in the BS box to lead to charge transport. On the contrary the β-sheet is about three times more efficient than the α-helix if we translate experimental β values into efficiencies.

To explain the higher efficiency of the β-sheet, we first show the FPTD of rigid β-sheet structure in azurin. Then, we confirm that in our calculations the solvated β-sheet has a weaker H-bond than an isolated one. This shows that our solvent model is working correctly here. This breaks the strong interaction between chains inside the β-sheet bound through the H-bond observed in the isolated case.

In Figure 6 we locally heat the residue 83 of azurin with E_{1667K} and count the successful run as the O−O distance larger than 4.0 Å. There is only one sharp peak in this figure. Hence, this is a result of the rigid structure of the β-sheet; here the result of no solvent being present. The carbonyl group does not flip away from its original position during the heating process.

Hydrogen-Bonded Structure. Since azurin contains a β-sheet structure, in refs 17 and 33, the redox active sites are attached to it and there are 30 amino acid residues between. Its β-value is ca. 1.0 $Å^{-1}$, and the charge transport efficiency is high. Instead of using such a long polypeptide chain, we choose a shorter model polypeptide chain from a synthesized β-sheet which consists of 12-mer acids, i.e. V_5PGV_5.[34] In a vacuum, MD shows this β-sheet to contain four hydrogen bonds (see Table 3). When it is dissolved in a 485 water cluster, it should be noted that the

TABLE 3: Hydrogen Bonds of V_5PGV_5[a] in the Gas Phase[b]

V_4-O	- - - -	$H-N-V_{10}$
$V_{12}-N-H$	- - - -	$O-V_2$
V_4-N-H	- - - -	$O-V_{10}$
$V_{12}-O$	- - - -	$H-N-V_2$

[a] The sequence of V_5PGV_5 is $Ace-V_1-V_2-V_3-V_4-V_5-P_6-G_7-V_8-V_9-V_{10}-V_{11}-V_{12}-NH_2$ ($Ace = -COCH_3$). [b] The hydrogen bond pair is expressed in terms of Aa ---- bB, where a and b are the atoms in residues A and B, respectively.

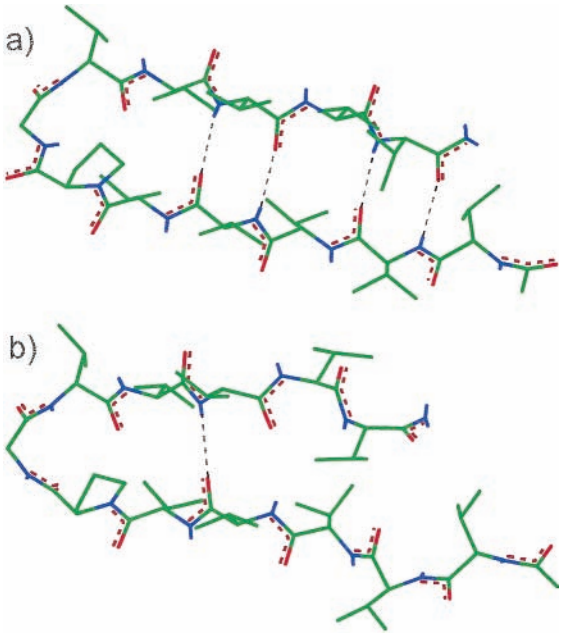

Figure 7. Hydrogen bond of V_5PGV_5 in a water system. (a) In a vacuum, the polypeptide contains four H-bond pairs. (b) When the sample is dissolved in water, the number of H-bonds is decreased and the bond energy is weaker.

number of hydrogen bond pairs is reduced and the bond length is increased, i.e., weakened (see the snapshot in Figure 7). Hence we interestingly observe directly the weakening of the H-bonded structure. As an example we pick up one hydrogen bond, for example 4O−10H, and measure its relevant first passage time for the hydrogen bond to dissociate through its FPTD curve (see Figure 8) at different temperatures. We take dissociation to occur when the bond is distended to a critical distance of 3.0 Å. At 300 K the first passage time for dissociation of the H-bond in water is ca. 65 fs. Alternatively, at 350 K, we have the first passage time ca. 46 fs. Estimating the H-bond bond strength from the activation energy by using the Arrhenius formula interestingly gives us the H-bond energy in water of ca. 1.70 kcal/mol. This computer experiment now directly includes effects from enthalpy and entropy, which is otherwise difficult to assess. In a nonaqueous environment this value rises to some 4.2 kcal/mol.[35] Correspondingly our MD results present an activation energy of some 4.7 kcal/mol. The enthalpy is typically calculated to be some 6 kcal/mol.[36] Hence, these MD computer experiments nicely demonstrate the known weakening of the H-bond in water,[35] as is required to ensure the chain mobility required for global processes such as folding since the higher energies would make such mobility quite difficult. This represents a cautionary note for dynamics calculations without water.

The dissolved β-sheet, thus, has much more flexibility than in a vacuum. This is even seen here in the structural MD simulations. The charge transport along each individual chain inside the β-sheet is seen to have the same efficiency as it has in the α-helix. But the sum of the efficiency of the β-sheet is the geometric sum of each individual chain. Hence, for the example azurin, the β-sheet contains about three chains. Its efficiency is expected to be about three times higher than that of each individual α-helix chain. We thus have an efficiency of the β-sheet ca. 0.0244; i.e., β-value $= 1.0$ Å^{-1}. Therefore, for the theoretical predicted collision distance for firing, the calculated efficiency here predicts a β-value that corresponds closely to that of known experiments.

In contrast to some intuitive views, this work suggests that charge transport in water is not necessarily optimal; charge transport in an isolated environment such as in the gas phase when energetically permitted is some 100-fold more efficient. The inefficiency in water is here attributed to a hydrophobic water barrel surrounding the peptide chain. This impedes the internal rotations which in our model are essential for charge transport. Here the theoretically calculated inefficiency agrees with experiment.

Conclusion

To summarize, local excitation in our bifunctional model based on two rotors motions around a C_α-hinge and the charge transfer occurring in an O−O atoms collision can be mapped into an escape process inside a subregion with a gate in the

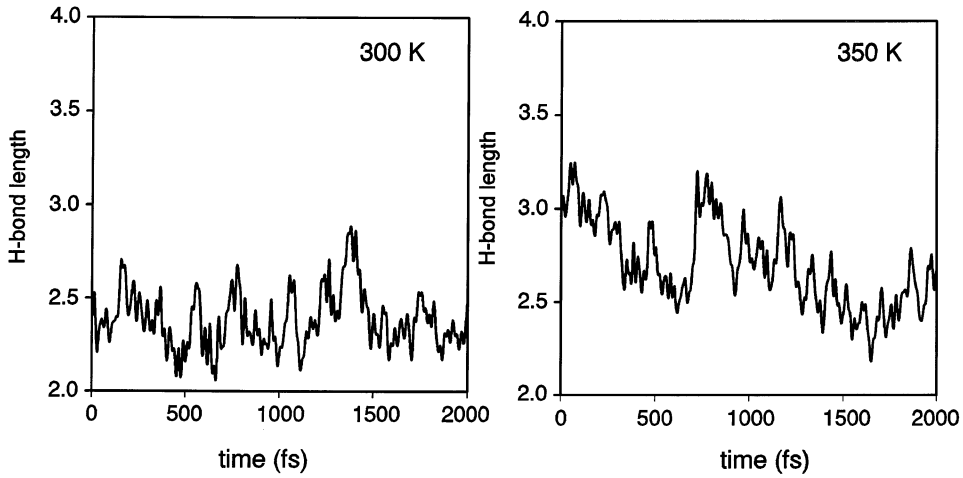

Figure 8. Hydrogen bond dissociation process. When V_5PGV_5 is dissolved in the water system, we measure the relative distance between H---O atoms vs time and the dissociation time is counted while H---O distance is equal to 2.5 Å. This dissociation time is noted as the first passage time for the hydrogen bond dissociation process.

bounds of the Ramachandran plot or the BS box. Before the charge is transferred, it waits in the C-side of C_α-hinge. Since it carries charge energy, the corresponding ψ angle is locally excited. By using MD simulation, we introduce a local excitation procedure which in MD generates the efficiency of successful collision between O−O atoms. The good agreement with the β-value between the simulation result and experimental data suggests the unique result that real protein charge transport depends heavily on protein dynamics. Since the 2D escape process is entropy driven and protein dynamics dominates the entire charge transport process, this is here seen as the charge transport generated in the restricted Ramachandran plot or BS box.

The model of mean first passage times and efficiency successfully survives the change in medium, which involves some 2 orders change in rate that must be predicted. Furthermore it can even be transferred to charge migration in secondary structures and displays strong differences between the α-helix and β-sheet. Interestingly the hopping rates are similar, but the efficiencies are grossly different. The β-sheet here is seen to be superior in charge transfer to the α-helix just as a result of parallel path and not intrinsically. Nevertheless water is interestingly seen as a strong impediment for charge migration here.

Acknowledgment. This work was supported by the Taiwan/Germany program at the NSC/Deutscher Akademischer Austauschdienst.

References and Notes

(1) Laidler, K. J. *Chemical Kinetics*; Harper & Row: New York, 1987.
(2) Zubarev, R. A.; Nielsen, M. L.; Budnik, B. A. *Eur. J. Mass. Spectrom.* **2000**, *6*, 235.
(3) Zubarev, R. A.; Kelleher, N. L.; McLafferty, F. W. *J. Am. Chem. Soc.* **1998**, *120*, 3265.
(4) Nielsen, M. L.; Budnik, B. A.; Haselmann, K. F.; Olsen, J. V.; Zubarev, R. A. *Chem. Phys. Lett.* **2000**, *330*, 558.
(5) Zubarev, R. A.; Kruger, N. A.; Fridriksson, E. K.; Lewis, M. A.; Horn, D. M.; Carpenter, B. K.; McLafferty, F. W. *J. Am. Chem. Soc.* **1999**, *121*, 2857.
(6) Budnik, B. A.; Zubarev, R. A. *Chem. Phys. Lett.* **2000**, *316*, 19.
(7) Lehninger, A. L.; Nelson, D. L.; Cox, M. M. *Principles of Biochemistry*; Worth Publishers: New York, 1998.
(8) Schlag, E. W.; Sheu, S.-Y.; Yang, D.-Y.; Selzle, H. L.; Lin, S. H. *Proc. Natl. Acad. Sci. U.S.A.* **2000**, *97*, 1068.
(9) Schlag, E. W.; Sheu, S.-Y.; Yang, D.-Y.; Selzle, H. L.; Lin, S. H. *J. Phys. Chem. B* **2000**, *104*, 7790.
(10) Sheu, She-Yi; Schlag, E. W.; Yang, Dah-Yen; Selzle, H. L. *J. Phys. Chem. A* **2001**, *105*, 6353.
(11) (a) Onuchic, J. N.; Beratan, D. N. *J. Chem. Phys.* **1990**, *92*, 722. (b) Onuchic, J. N.; de Andrade, P. C. P.; Beratan, D. N. *J. Chem. Phys.* **1991**, *95*, 1131.
(12) (a) Siddarth, P.; Marcus, R. A. *J. Phys. Chem.* **1993**, *97*, 2400. (b) Siddarth, P.; Marcus, R. A. *J. Phys. Chem.* **1993**, *97*, 6111.
(13) Ramachandran, G. N.; Sasisekharan, V. *Adv. Protein Chem.* **1968**, *23*, 283.
(14) Mayo, S. L.; Ellis, W. R., Jr.; Crutchley, R. J.; Gray, H. B. *Science* **1986**, *233*, 948.
(15) Crutchley, R. J.; Ellis, W. R., Jr.; Gray, H. B. *J. Am. Chem. Soc.* **1985**, *107*, 5002.
(16) Kostic, N. M.; Margalit, R.; Che, C.-M.; Gray, H. B. *J. Am. Chem. Soc.* **1983**, *105*, 7765.
(17) Gray, H. B. *Chem. Soc. Rev.* **1986**, *15*, 17.
(18) Isied, S. S.; Kuehn, Ch.; Worosila, G. *J. Am. Chem. Soc.* **1984**, *106*, 1722.
(19) Nocera, D. G.; Winkler, J. R.; Yocom, K. M.; Bordignon, E.; Gray, H. B. *J. Am. Chem. Soc.* **1984**, *106*, 5145.
(20) Winkler, J. R.; Gray, H. B. *JBIC* **1997**, *2*, 399.
(21) Langen, R.; Chang, I.-Jy; Germanas, J. P.; Richards, J. H.; Winkler, J. R.; Gray, H. B. *Science* **1995**, *268*, 1733.
(22) Beratan, D. N.; Onuchic, J. N.; Betts, J. N.; Bowler, B. E.; Gray, H. B. *J. Am. Chem. Soc.* **1990**, *112*, 7915.
(23) Beratan, D. N.; Onuchic, J. N.; Winkler, J. R.; Gray, H. B. *Science* **1992**, *258*, 1740.
(24) (a) McConnell, H. M. M. *J. Chem. Phys.* **1961**, *35*, 508. (b) Miller, J. R.; Beitz, J. V. *J. Phys. Chem.* **1981**, *74*, 6746. (c) Nitzan, A.; Jortner, J.; Wilkie, J.; Burin, A. L.; Ratner, M. A. *J. Phys. Chem. B* **2000**, *104*, 5661. (d) Berlin, Y. A.; Burin, A. L.; Ratner, M. A. *J. Phys. Chem. A* **2000**, *104*, 443. (e) Ratner, M. *Nature* **1999**, *397*, 480.
(25) Brooks, B. R.; Bruccoleri, R. E.; Olafson, B. D.; Swaminathan, D. J.; States, S.; Karplus, M. *J. Comput. Chem.* **1983**, *4*, 187.
(26) Hu, Y.; Mukamel, Sh. *J. Phys. Chem.* **1989**, *91*, 6973.
(27) Rajski, S. R.; Kumar, S.; Roberts, R. J.; Barton, J. K. *J. Am. Chem. Soc.* **1999**, *121*, 5615.
(28) Meggers, E.; Michel-Beyerle, M. E.; Giese, B. *J. Am. Chem. Soc.* **1998**, *120*, 12950.
(29) Jortner, J.; Bixon, M.; Langenbacher, Th.; Michel- Beyerle, M. E. *Proc. Natl. Acad. Sci.* **1998**, *95*, 12759.
(30) Wan, Ch.; Fiebig, T.; Kelley, Sh. O.; Treadway, Ch. R.; Barton, J. K.; Zewail, A. H. *Proc. Natl. Acad. Sci. U.S.A.* **1999**, *96*, 6014.
(31) Barnett, R. N.; Cleveland, Ch. L.; Joy, A.; Landman, U.; Schuster, G. B. *Science* **2001**, *294*, 567.
(32) Kurnikov, I. V.; Tong, G. S. M.; Madrid, M.; Beratan, D. N. *J. Phys. Chem. B* **2002**, *106*, 7.
(33) Ponce, A.; Gray, H. B.; Winkler, J. R. *J. Am. Chem. Soc.* **2000**, *122*, 8187.
(34) Ferrara, P.; Apostolakis, J.; Caflisch, A. *J. Phys. Chem. B* **2000**, *104*, 5000.
(35) Klotz, I. M.; Franzen J. S. *J. Am. Chem. Soc.* **1962**, *84*, 3461.
(36) Davis, A. M.; Teague, S. J. *Angew. Chem., Int. Ed.* **1999**, *38*, 736.